JOURNAL OF MATERIALS SCIENCE 25 (1990) 5147–5156

# Electron diffraction and HREM studies of the new phase and superstructures in $Ca_4Al_6SO_{16}$

Y. G. WANG, H. Q. YE, K. H. KUO, X. J. FENG*, G. L. LAO*, S. Z. LONG*
*Laboratory of Atomic Imaging of Solids, Institute of Metal Research, Academia Sinica, Shenyang 110015, People's Republic of China*

The fine structure of unhydrated cement clinker $Ca_4Al_6SO_{16}$ ($C_4A_3S$) and its four superstructures have been studied by means of electron diffraction and high resolution electron microscopy (HREM). The match between experimental images and simulated ones verifies the result of X-ray structural analysis: $C_4A_3S$ having a cubic lattice with space group $I_{\bar{4}3m}$, $Z = 2$. The frequent apperance of forbidden reflections such as $\frac{1}{2}$, $-\frac{1}{2}$, 0 along the $\langle 1\,1\,0\rangle^*$ directions of $C_4A_3S$ imply the presence of superstructures which may be due to an orderly inverse occupation of $Ca^{2+}$ ions. Various structure models based upon the observed structural images have been proposed for these four superstructures. A new cubic phase with $a' = 1.5$ nm is also found by selected area electron diffraction (SAED).

## 1. Introduction

In 1957 a new cement of calcium aluminosulphate ($Ca_4Al_6SO_{16}$, usually abbreviated as $C_4A_3S$) was first reported by Ragozina [1] and has since then been extensively studied. $C_4A_3S$ is the only ternary compound detected in the cement of $CaO$–$Al_2O_3$–$SO_3$ system and its stability is unusual. This cement with excellent hydraulicity and greatly expanding in application is of potential commercial interest in cement manufacture. It can be hydrolysed rapidly by water to form predominantly calcium aluminate hydrates and it is therefore unlikely to occur naturally, although structurally it may be regarded as an end member of the sodalite–hauyanite series of naturally occurring minerals. The structure of $C_4A_3S$ was first analysed by Halstead and Moore [2] using X-ray powder diffraction and their result showed that it has a similar arrangement of atoms as ultramarine and its Bravais lattice belongs to the b.c. cubic unit with unit cell parameter of about 0.9 nm. The examination of atom positions in the unit cell was not carried out because it is difficult to obtain single crystals large enough for the X-ray or neutron diffraction. Recently Feng *et al.* [3] have determined the atomic positions by using four-circle X-ray diffractometer for $C_4A_3S$ single crystal with size larger than 0.1 mm in linear dimension and their result is shown in Table I.

Previous X-ray diffraction data sometimes showed superlattice reflections such as $\frac{1}{2}\frac{1}{2}0$ and $\frac{1}{2}\,-\frac{1}{2}0$ etc. implying the existence of superstructures in this cement clinker, but no detailed study has been made.

HREM is well-suited for the study of fine structures and defects of cement because it permits one to image non-periodic features. The resolution power attainable in modern instruments allows details to be seen on extremely fine scales, even within unit cells or at the atomic level [4, 5] and during the past few years there have been many studies that have utilized this technique of HREM to investigate cement clinker [6].

In the present study the structure of $C_4A_3S$ and its four superstructures have been studied at atomic level by HREM and various structure models with an ordered inverse occupation of calcium atoms have been proposed for these four superstructures. The SAED also shows the presence of a new cubic phase with lattice parameter of about 1.5 nm in this cement.

## 2. Experimental details

The synthetic compound $C_4A_3S$ was prepared by mixing calcium oxide, oxide of alumina and a calcium sulphate according to the proportion of $3CaO : 3Al_2O_3 : CaSO_4$ and pressing the powder mixture in a cylindrical mould at 150 MPa. The resultant compact pieces (diameter about 20 mm and thickness about 10 mm) were finally heated in the platinum container in a platinum–rhodium-wound alumina muffle furnace. No special steps were taken to control the furnace atmosphere, but evidence from other preparations for which the furnace had been used showed that reducing conditions were unlikely to occur. It was found from the results of the X-ray diffraction [2] that the reaction went to completion at about 1350° C and therefore the mixture was sintered at 1380° C for 8 h. The sintered specimen was then cooled after withdrawal from the furnace and examined by X-ray diffraction. The preparation was a little yellowish white and brittle so that it could be ground into thin fragments in an agate mortar, and then was made into a suspension in absolute alcohol by supersonic vibration in order to disperse these fragments as uniformly as possible in alcohol. A drop of this suspension was scooped onto copper grids coated with holey carbon film and the

*Also at Wuhan University of Technology, Luoshi Road 14, Wuhan, P.R. China.

0022–2461/90 $03.00 + .12 

TABLE I Atom positions, parameters and occupations in $Ca_4Al_6SO_{16}$

| Atom | Position | $x$ | $y$ | $z$ | Occupation |
|---|---|---|---|---|---|
| CaI | 8c | 0.1904 | 0.1904 | 0.1904 | ~3/4 |
| CaII | 8c | 0.2422 | 0.2422 | 0.2422 | ~1/4 |
| S | 2a | 0.0000 | 0.0000 | 0.0000 | 1 |
| Al | 12d | 0.2500 | 0.2500 | 0.2500 | 1 |
| OI | 8c | 0.4040 | 0.4040 | 0.4040 | 1 |
| OII | 24g | 0.1520 | 0.1520 | 0.4450 | 1 |

specimen was examined with a JEM-200CX electron microscope equipped with a top-entry goniometer stage and an ultra-high resolution pole piece (Cs = 1.2 mm) having an interpretable resolution of 0.25 nm. Composition analysis was carried out in a Phillips 400T electron microscope with an EDAX 9100 X-ray energy-dispersive spectrometer and standard thin-film correction software supplied by the maker was used. In observation various crystals with ⟨1 0 0⟩, ⟨1 1 0⟩ and ⟨1 1 1⟩ orientations were chosen so that the images always include one or two, or even three ⟨1 1 0⟩ directions, which made it easier to identify the superstructures along these directions. All high resolution images were taken as much as possible taken under the symmetrical incidence condition in order to compare with the results of image simulation. A low beam current density was used in the observation since $C_4A_3S$ is sensitive to the electron beam irradiation and the image intensifier was also used in order to solve this problem.

## 3. Structure images of the $C_4A_3S$ matrix

The structure model of $C_4A_3S$ projected on (0 0 1) is shown in Fig. 1a, in which there are two sets of 8c position in $I_{\bar{4}3m}$, namely CaI and CaII, occupied by the calcium atoms, respectively, and the ratio of occupations in these two sets of positions is about 3 : 1 [3]. This suggests that the calcium atoms can freely occupy these sets in various degree and usually they almost all locate on the CaI positions. Such cases also mean calcium can move along the body diagonals of the unit cell in $C_4A_3S$ or deviate from the equilibrium positions (CaI) to the same extent.

In order to interpret the observed high resolution images unambiguously, simulated images were calculated based upon the multislice program written by Ishizuka [7]. The optimum defocus value of − 65.0 nm corresponding to the first broad band in the transfer function for Cs = 1.2 mm at an accelerating voltage of 200 kV was used. By calculating the variation in the statistically independent fluctuations in accelerating voltage and objective current, the half-width of a Gaussian spread of defocus is 70 nm at the experimental gun bias. The semi-angle of convergence of the incident beam, $\theta c/\lambda = 0.30\,\mathrm{rad\,nm^{-1}}$, can be estimated from a focused condenser aperture diffraction pattern. The size limited by the objective aperture, $(\sin\theta)/\lambda = 0.35\,\mathrm{nm^{-1}}$, can be measured from a double-exposed diffraction pattern. A through-focus series of the lattice images were found in good agreement with the simulated ones. Figs 1b and 2 are a pair of them at Scherzer defocus for a thickness of 4.5 nm, where each bright spot in the images corresponds to a column of sulphur atoms in the structure model (Fig. 1a). The through-focus series of high resolution images along the other directions were also taken and they all well match with the simulated ones. Figs 3 and 4 show the [1 1 1] structural projection, a series of simulated images calculated at a thickness of 45 nm and experimental images, respectively, in which it can be seen that the positions and contrast of the bright dots in the calculated images will change with an increase in defocus values. No matter how the change of contrast occurs in simulated images, the bright dots in the observed and simulated images accord with each other not only in position but also in orientation. The bright dots taken at different defocus values correspond very well with the tunnels formed by the oxygen atoms or the columns of overlapped sulphur, oxygen and calcium atoms located at corners of projected unit cell in Fig. 3a, respectively. Therefore the result of X-ray examination has been proved to be creditable by the

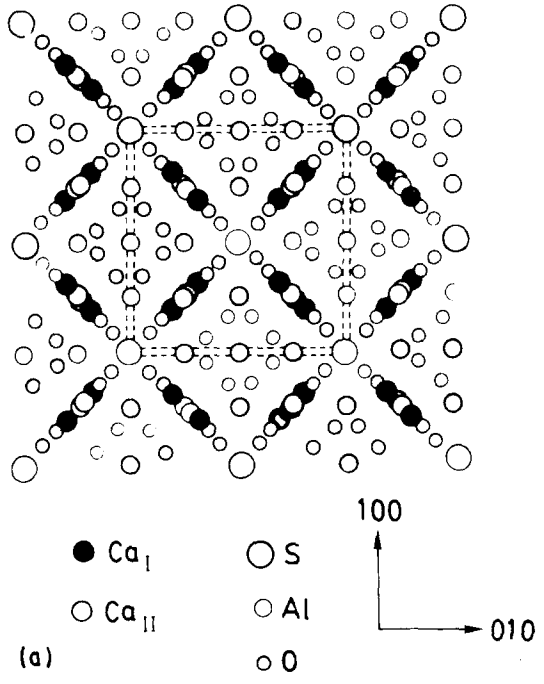


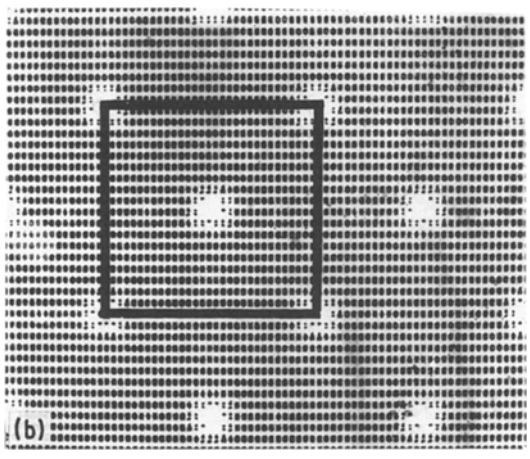


*Figure 1* (a) Schematic projection of $C_4A_3S$ along the [0 0 1] direction and (b) a simulated image calculated at a thickness of 45 nm and the Scherzer defocus ($\Delta f$ = −60.0 nm) shows good correspondence of bright dots and sulphur atoms columns in the structure.

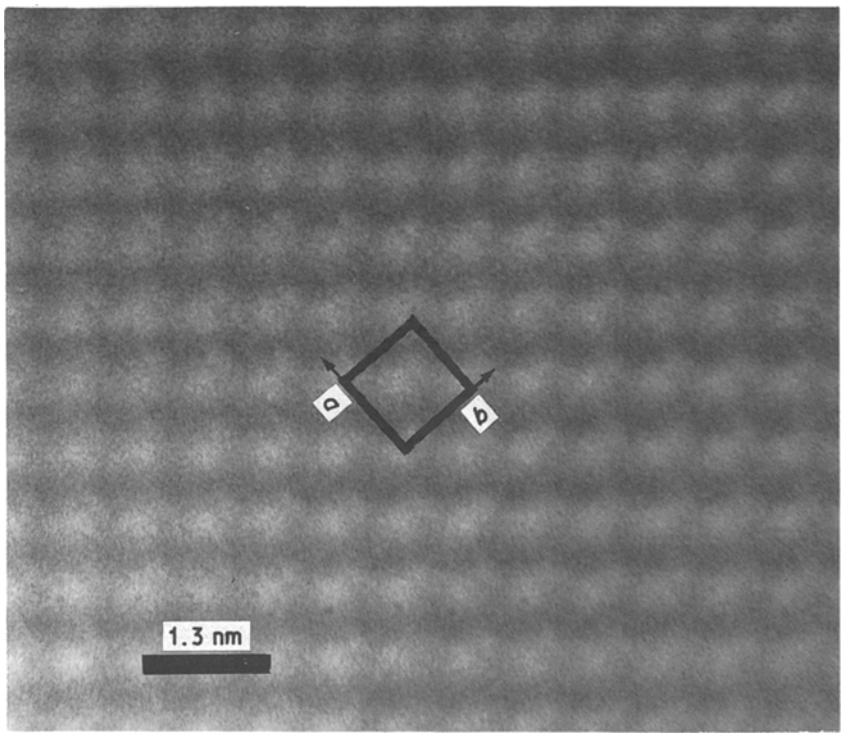


*Figure 2* The [0 0 1] structural image of $C_4A_3S$ taken at the Scherzer defocus.

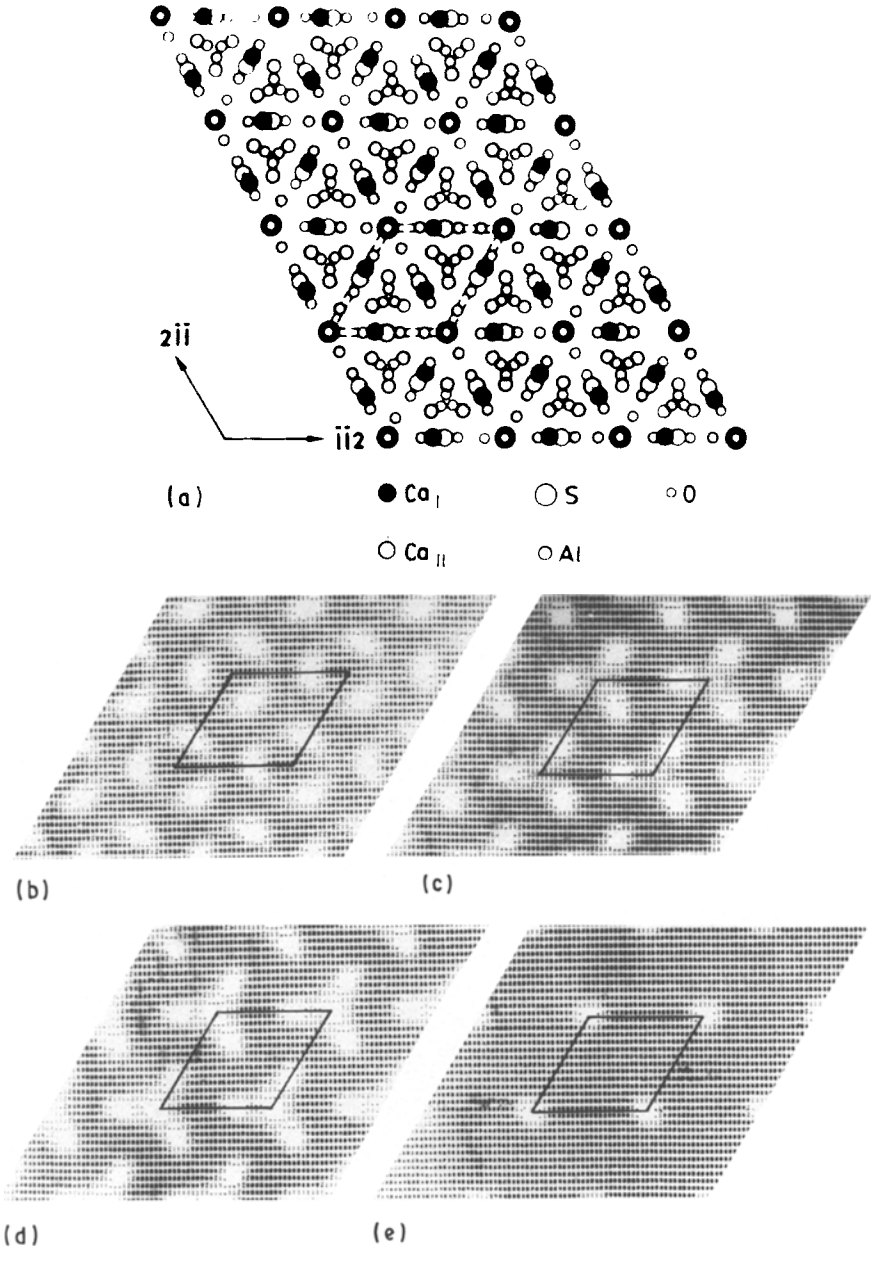


*Figure 3* (a) Structure of $C_4A_3S$ projected on (1 1 1) and (b) to (e) the series of simulated images calculated from a crystal with thickness of 5.0 nm (b) 48 nm, (c) 55 nm, (d) 65 nm, (e) 75 nm.

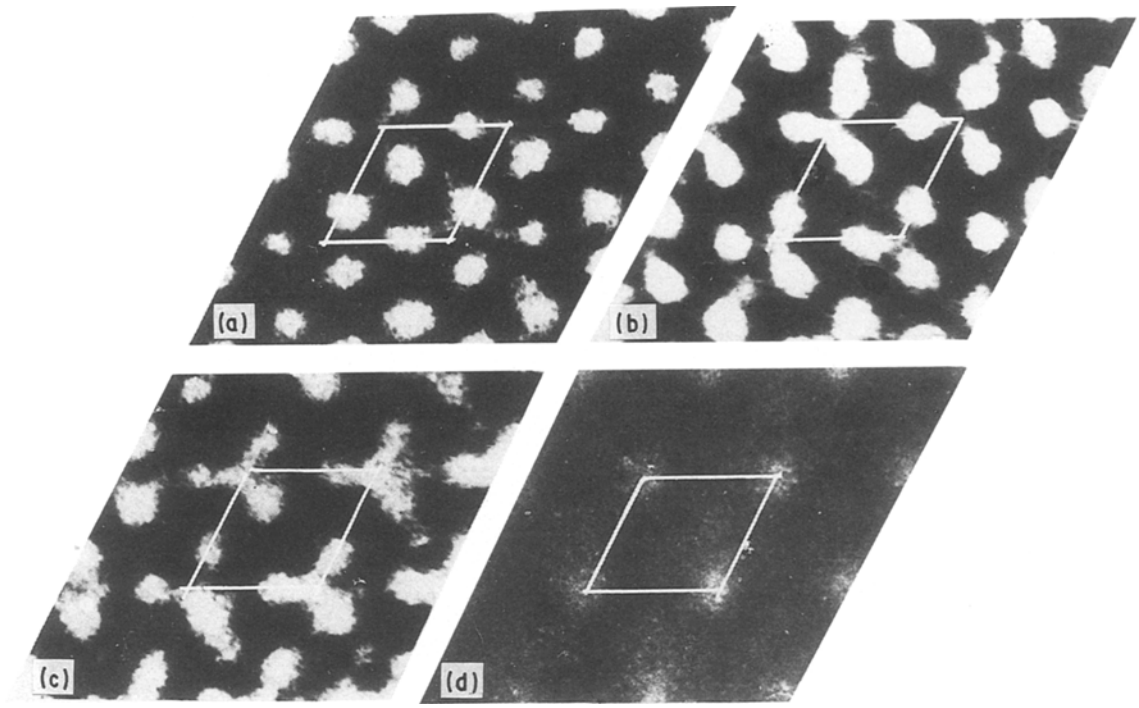


*Figure 4* The through-focus series of the [1 1 1] structural images of $C_4A_3S$.

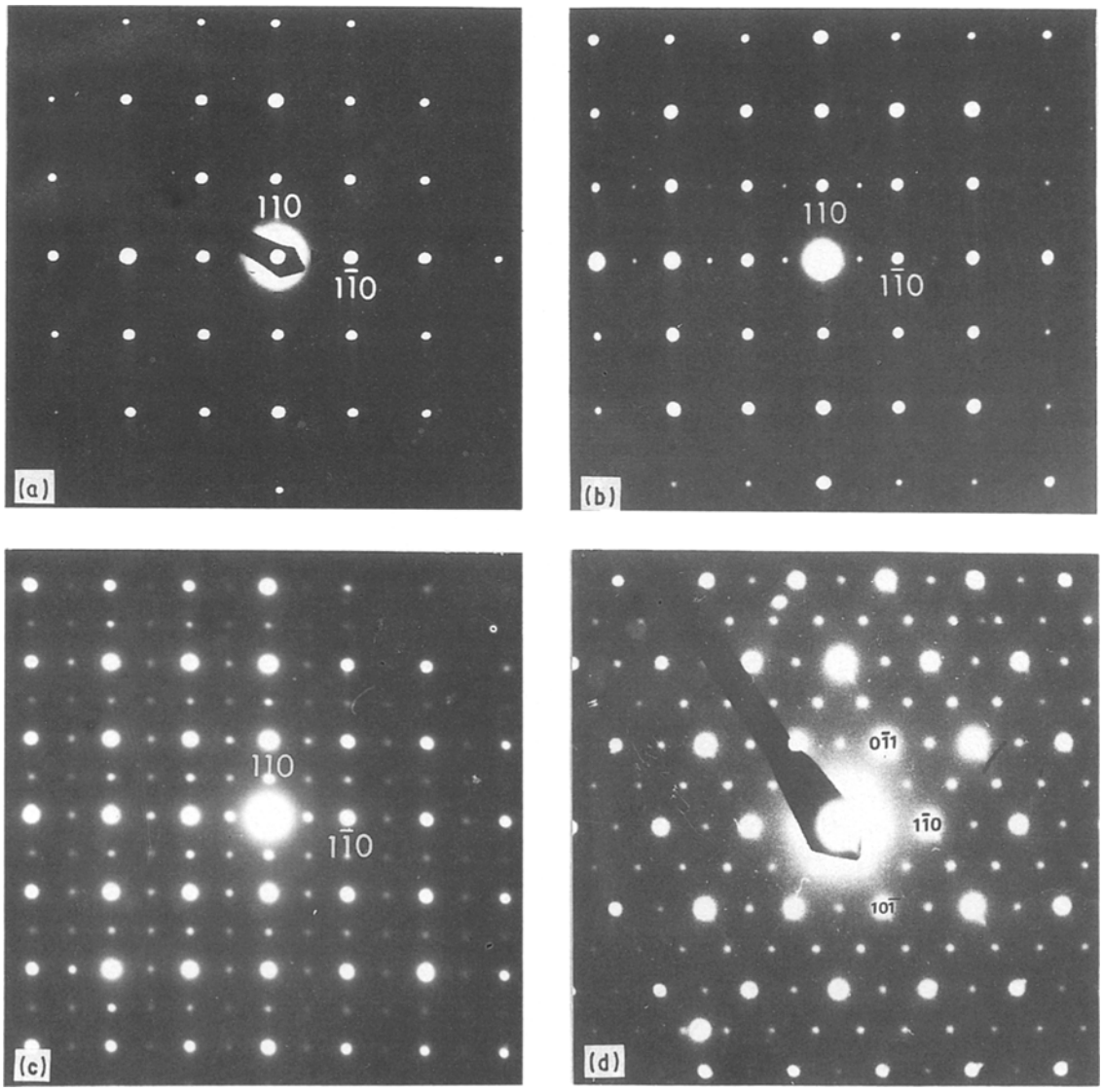


*Figure 5* The electron diffraction patterns of (a) $C_4A_3S$ matrix and the three superstructures: (b) 1D, (c) 2D and (d) 3D. Fractional spots at $\frac{1}{2}\frac{1}{2}0$, $\frac{1}{2}-\frac{1}{2}0$ etc. correspond to the superlattice reflections.

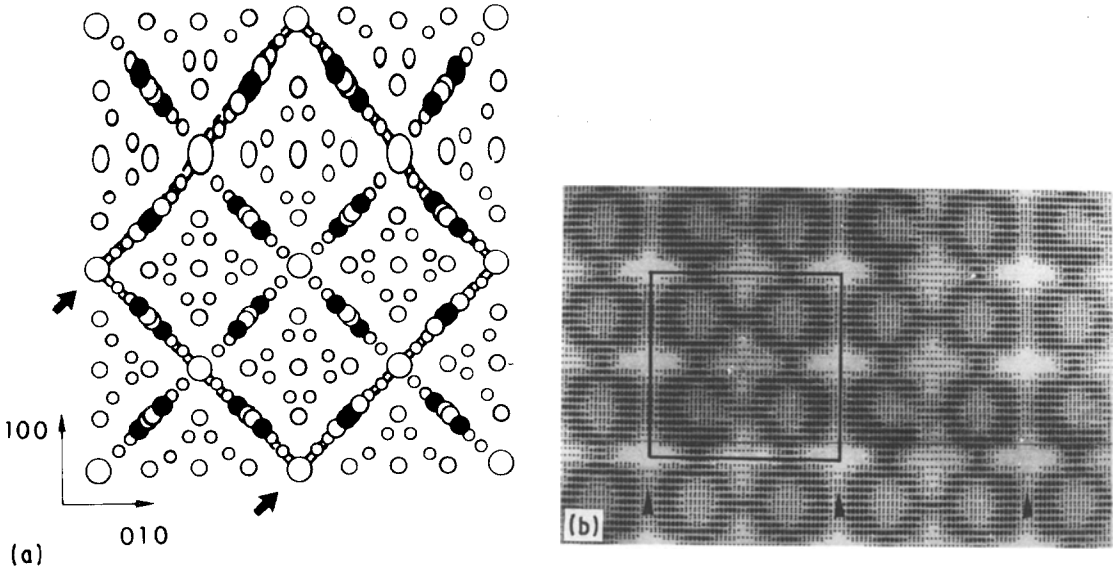


*Figure 6* (a) A possible structure model of 1D superstructure projected on (0 0 1) and (b) a simulated image calculated at a thickness of 45 nm and the Scherzer defocus.

coincidence of simulated and observed image and such a good correspondence in the case of the well established structure of $C_4A_3S$ suggests that the structural image taken at the Scherzer defocus could be used to interpret the superstructures of $C_4A_3S$.

## 4. Superstructures with ordered inverse occupation of calcium atoms

### 4.1. Superlattice reflections

The superstructure can be derived from a simple structure by introducing some periodic modifications, i.e. planar interfaces stacking faults, or anti-phase boundaries. It could also be caused by the periodic composition variation, for instance the periodic variation in the filling of a certain family of planes of interstice atoms. Thus the extra reflection could result. As mentioned above, superlattice reflections along the $\langle 1\,1\,0\rangle$ directions occur frequently in $C_4A_3S$ implying the presence of ordered inverse occupation of calcium atoms with two times of the fundamental period. Figure 5 shows the electron diffraction patterns from the fundamental structure as well as those three superstructures. There are fractional spots at $\frac{1}{2}$ along the $[1\,\bar{1}\,0]$ direction in Fig. 5b showing one dimensional feature, wheras along the two $\langle 1\,1\,0\rangle$ directions in Fig. 5c and three $\langle 1\,1\,0\rangle$ directions in Fig. 5d showing two and the three dimensional features, respectively. We call these three superstructures one dimensional (1D), two dimensional (2D) and three dimensional (3D) superstructures in turn.

### 4.2. 1D superstructure

In the fundamental structure the $SO_4^{2-}$ clusters are in more stable positions than those of calcium so that the superstructure could be caused by the periodic occupations of calcium atoms and thus various structure models of this superstructure may be derived from the basic one owing to the different ordering occupations of calcium atoms on the two sets of positions. Fig. 6a shows one possible structure, in which the periodic inverse occupations of calcium ordering occurring on the $(1\,\bar{1}\,0)$ plane in an alternate

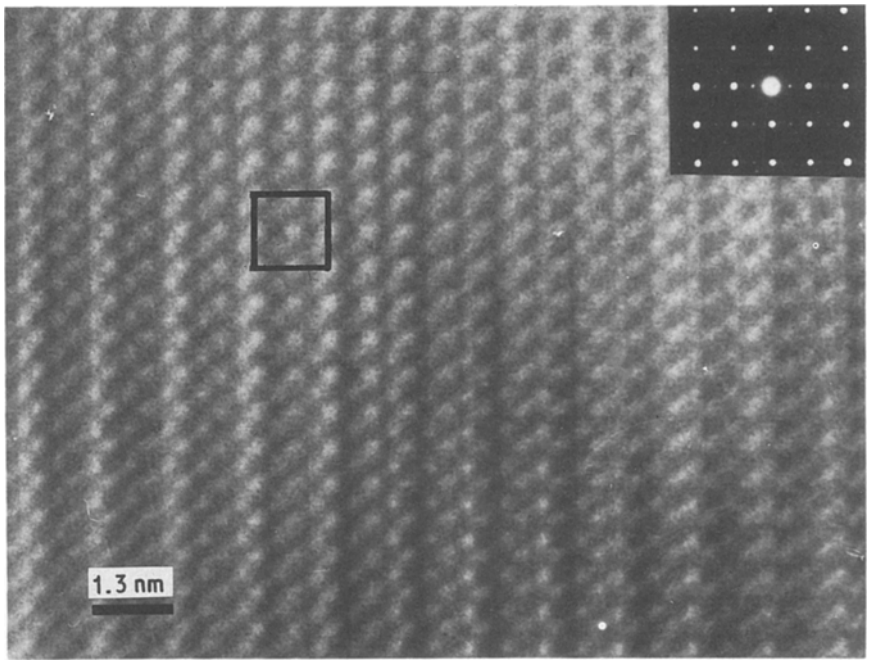


*Figure 7* The [0 0 1] structural image of 1D superstructure taken at the Scherzer defocus.

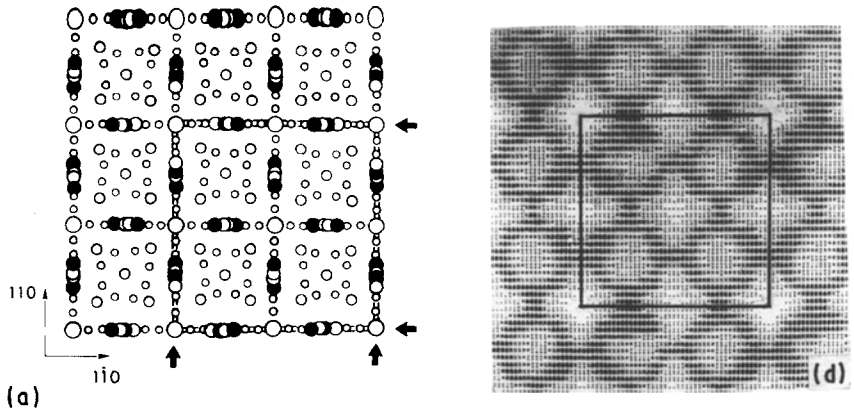


*Figure 8* (a) A possible structure model of 2D superstructure projected on (0 0 1) and (b) a simulated image calculated at the same conditions as Fig. 5b.

way so that the long periods of $2^{*}d_{1\bar{1}0}$ is formed. In this process, small deviation of partial oxygen atoms may be introduced as well. The simulated images were calculated for several models with different occupations of calcium atoms on two sets of positions for varying defocus and thickness. It was found that the simulated image based on the model with inverse occupation of calcium which has been shown in Fig. 6a shows the best agreement with the experimental one, and this simulated image is shown in Fig. 6b which is calculated with 528 waves at a crystal thickness of 45 nm assuming symmetrical incidence. The difference of contrast between the dots is exhibited very clearly, i.e. the dots on the plane where inverse occupation happened become brighter than those on the unchanged plane. This simulated image shows a good match with the experimental image (Fig. 7) taken at the thin edge of crystallite under nearly the same conditions as the simulated one, in which the 1D superstructure can be clearly seen. The matches between the simulated and observed images of 1D superstructure in different orientations are all very well and the increase in contrast of bright dots seems to be related with the increase in occupation of calcium on CaII positions. The one to one correspondence between the bright dots in the observed and simulated images supports the correctness of the given structure model (Fig. 6a), and we believe that the superstructure in $C_4A_3S$ are actually related to the different periodic occupations of calcium. The arrangement of CaI and CaII positions with the different occupations of calcium in the 1D superstructure destroys the symmetry of the basic structure, for example 3-fold symmetry along the $\langle 1\,1\,1 \rangle$ axes may be lost, so that the phase transformation

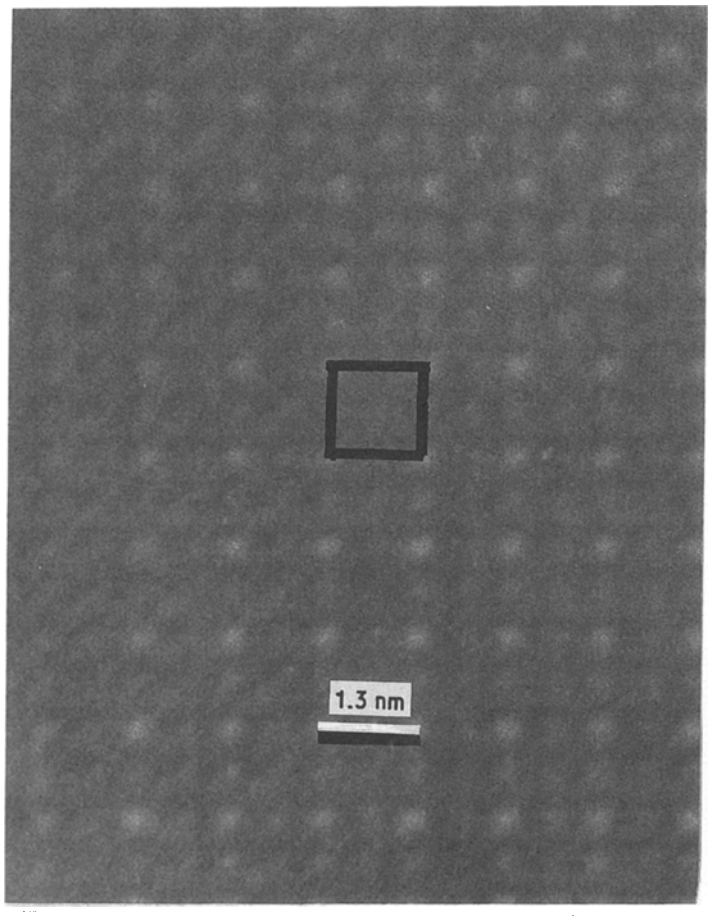


*Figure 9* The [0 0 1] structural image showing 2D superstructure.

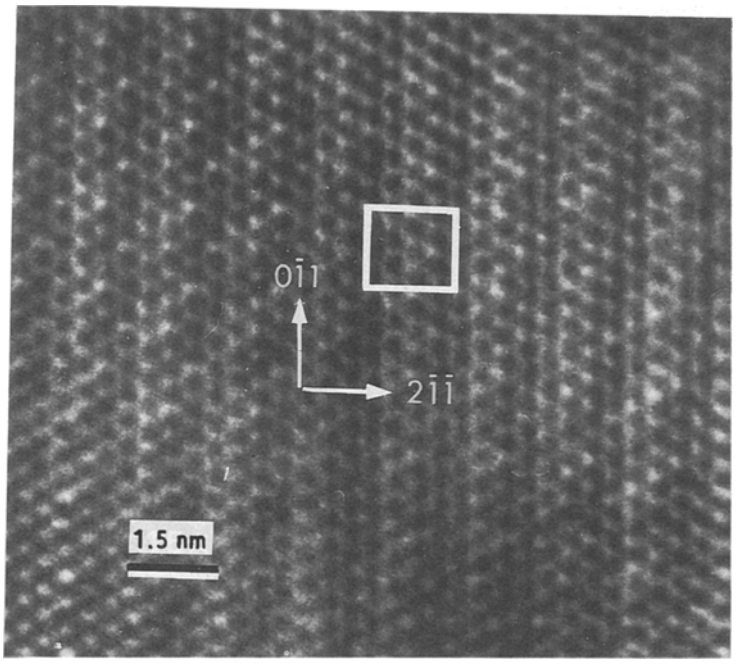


*Figure 10* The [1 1 1] structural image showing another 2D superstructure, the double repeat periods along the [0 $\bar{1}$ 1] and [2 $\bar{1}$ $\bar{1}$] directions can clearly be seen.

would also be introduced. The unit cell of this 1D superstructure derived from the structure model (Fig. 6a) is B centred orthorhombic with $a = 1.298$, $b = 1.298$, $c = 0.919$ A, $Z = 4$ and the possible space group is Bmm2. The orientation relationship of 1D superstructure and fundamental one is; $a' \| [1\,1\,0]$, $b' \| [1\,\bar{1}\,0]$, $c' \| [0\,0\,1]$.

### 4.3. 2D superstructure

The structure model (Fig. 8a) of 2D superstructure could also be derived from the fundamental structure by introducing periodic occupation of calcium on two sets of positions in a similar way as shown in Fig. 6a in which the double periodic of $d_{1\,1\,0}$ along the [1 1 0] and [1 $\bar{1}$ 0] directions are introduced. Fig. 8b shows the simulated image calculated with 830 waves at the same crystal thickness as Fig. 5b and Fig. 9 is the experimental high resolution image of such superstructure taken at the wedge portion of crystallite with the thickness of about 5.0 nm in the image simulation. The match between the calculated and observed image is reasonably good and thus suggests that the proposed structure model may be creditable to some extent. Considering the symmetrical distributions of the CaI and CaII sites with different occupations of the calcium, thus its unit cell is tetragonal although the lengths of axes and the orientation relationship with the fundamental structure are the same as those of the 1D superstructure and the possible space group of 2D superstructure can be decided as P$\bar{4}$m2. Consequently the phase transformation from cubic to tetragonal might be introduced in this case.

Another superstructure with a 2D feature is shown in Fig. 10, in which the double repeat periods along the [0 $\bar{1}$ 1] and [2 $\bar{1}$ $\bar{1}$] directions can be detected. The possible structure model of this superstructure could be suggested in a similar way as above and shown in Fig. 11, where periodic inverse occupation on CaII positions is presented only along one body diagonal so that this superstructure may be monoclinic with $a' = 1.592$, $b' = 1.298$, $c' = 0.919$ nm, $\beta' = 125°16'$, and the orientation relationship with the basic structure

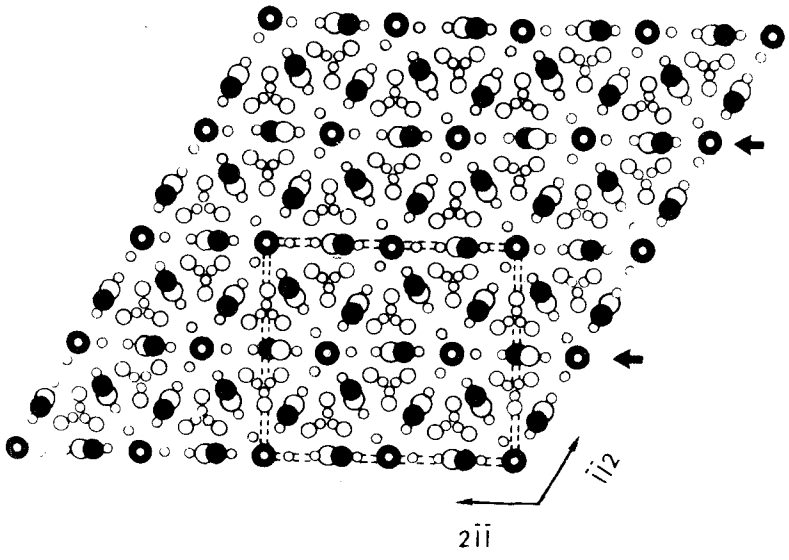


*Figure 11* A possible structure model of 2D superstructure (see Fig. 10) projected on the (1 1 1) plane.

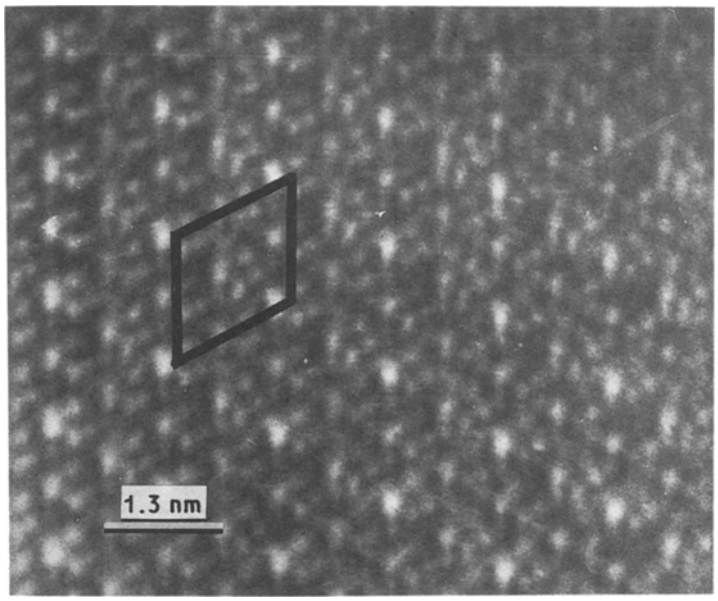


*Figure 12* The [1 1 1] structural image of 3D superstructure.

are; $a' \| [1\,\bar{1}\,\bar{1}]$, $b' \| [0\,\bar{1}\,1]$, $c' \| [\bar{1}\,0\,0]$. The phase transformation from cubic to monoclinic could also be caused on this case.

### 4.4. 3D superstructure

A superstructure with $a = 2{*}a$ has also been mentioned earlier though no detailed information was given [2, 3]. The electron diffraction pattern of this superstructure has already been given in Fig. 5d, and Fig. 12 shows the corresponding high resolution image, in which the double periodicities along the three $\langle 1\,\bar{1}\,0 \rangle$ direction can be seen more clearly. From the above discussion it has been shown that the different contrast may be caused by the inverse occupations of calcium and therefore the structure model of such superstructure can be shown as in Fig. 13, which is constructed by the ordering arrangement of CaI and CaII sites with different occupations of the calcium atoms along the three or four diagonals of the unit cell in the matrix. Because these diagonals are not on the same plane or a family of parallel planes, this superstructure actually corresponds to the three dimensional case. Based upon this model, the space group can be pointed out to be $R_3$ for inverse occupation of calcium along the three diagonals. In this case the unit cell of the 3D superstructure is triagonal with $a' = 1.592\,\text{nm}$, $\alpha' = 109°28'$ and $a' \| \langle 1\,1\,1 \rangle$ so that the phase transformation from cubic to rhombohedral may be introduced.

Up to now the four superstructures related to different occupations of the calcium along the one, two and three or four body diagonals, respectively, have been proved to be present in $C_4A_3S$, which support the presence of different occupations of calcium or the periodic movement of calcium cations along the diagonals in this cement.

## 5. A new cubic phase

Although the most abundant phases examined in this cement are the body centred cubic phase with $a = 0.919\,\text{nm}$ and its various superstructures, another new phase was also detected. Figs 14a to c show a set of large angle tilted EDPs and Fig. 14d is the convergent beam electron diffraction pattern in the same orientation as Fig. 14b, in which there are three reflection mirrors indicated and thus the 3-fold symmetry in this direction is certainly confirmed. Therefore the Bravais lattice of this new phase can be determined to

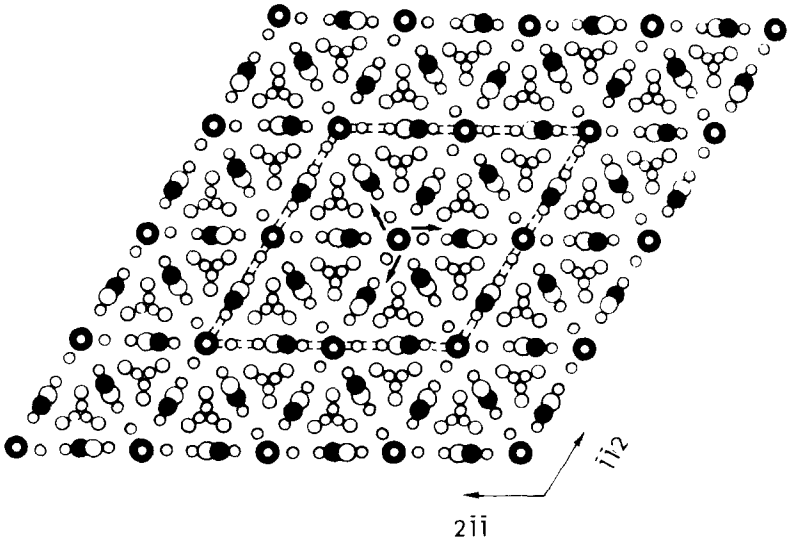


*Figure 13* A possible structure model of 3D superstructure projected on the (1 1 1) plane.

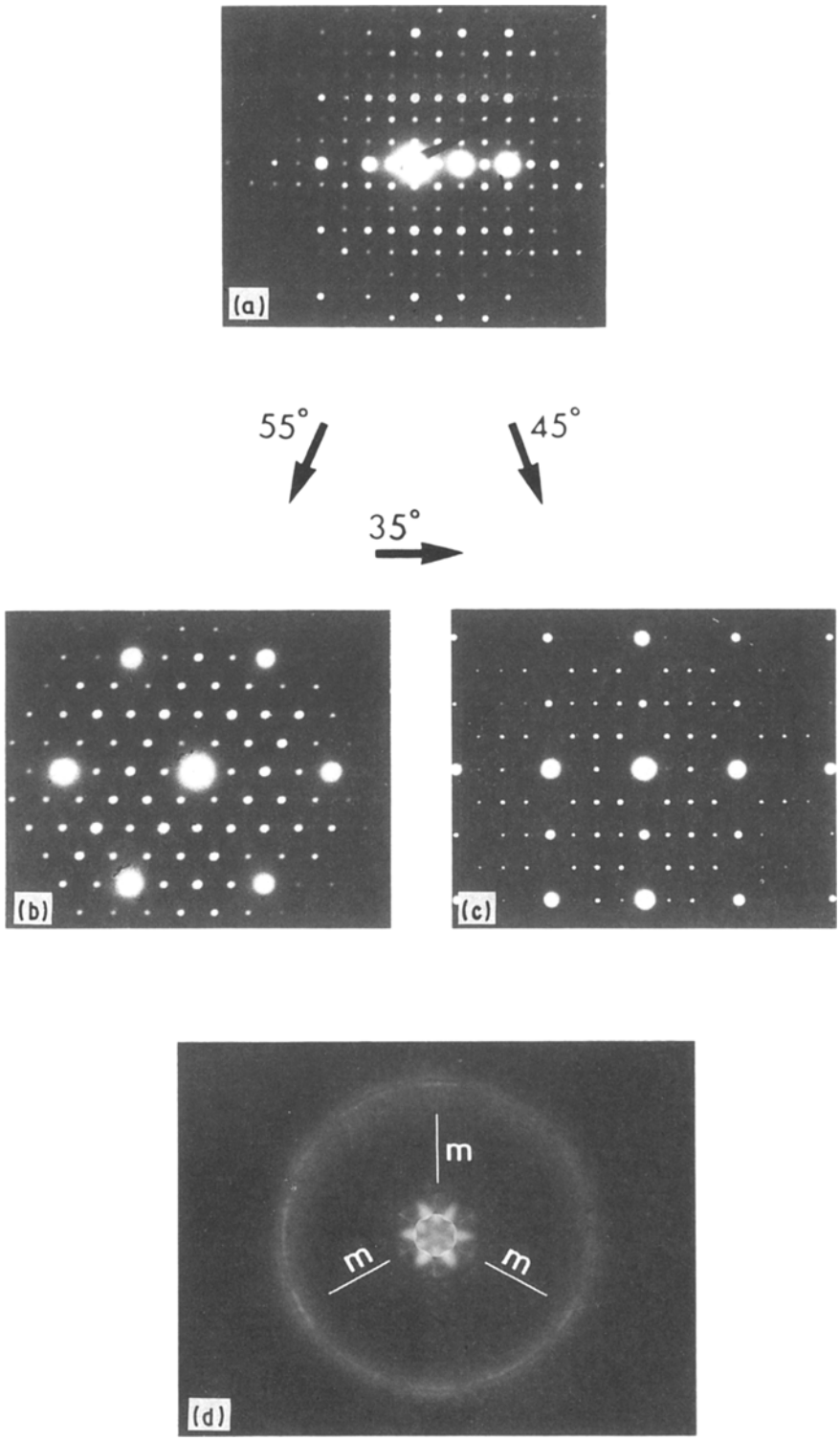


*Figure 14* Electron diffraction patterns from a newly found cubic phase on $C_4A_3S$. (a) to (c) showing a set of large angle tilt EDPs, which correspond to the [0 0 1], [0 1 1] and [1 1 1] zones, respectively, the distance between transmission spot and nearest diffraction spot in (a) corresponds to an interplanar spacing of 15 nm. (d) The convergent beam electron diffraction pattern with the same orientation as (b) showing 3-fold symmetry.

be a primitive cubic and the lattice parameter measured in Fig. 14a is about 1.5 nm. Qualitive estimation of EDAX on this phase shows it has nearly the same composition as the matrix so that it can be suggested that there may be a different phase co-existing with this cement clinker. Such a cubic phase can not be derived directly from the basic one and thus it must have a different arrangement of atoms from the fundamental structure.

## 6. Conclusion

The observation of the structural features on the level of the sub-unit cell provided insight into the chemical process. The details on the arrangement of atoms in this cement obtained by using the technique of HREM are helpful to study the phase transformation and the mechanism of solid state reactions involving the movements and mass transfer of atoms that are commonly problematical. The 1D, 2D and 3D

superstructures related to the periodic occupation of calcium are revealed and explained by comparing the experimental results with the simulated images of various suggested structure models. Moreover, a new cubic phase has also been detected. The discovery and characterization of the structural variations, that may be presumably intermediate products formed along the path of reaction in the preparation, have shown that $C_4A_3S$ is a much more complex compound than has previously been recognized. Computed images also enable us to determine the imaging effects resulting from the structural change in atom positions or occupancy in the specimen. By using the technique of HREM to study the cement yields an entirely new range of observations.

## References


1. T. A. RAGOZINA, *Zh. Prikl. Khin.* **30** (1957) 1682.
2. P. E. HALSTEAD and A. E. MOORE, *J. Appl. Chem.* **12** (1962) 413.
3. X. J. FENG, G. L. LAO and S. Z. LONG, *J. Chinese Silicate Society* (in Chinese) (in press).
4. P. R. BUSRCK and D. R. VRLEN, *Bull. Min.* **104** (1981) 249.
5. K. H. KUO, H. Q. YE and D. X. LI, *J. Electron Microscopy Technol.* **3** (1986) 57.
6. Y. G. WANG, B. S. ZOU and K. H. KUO *et al.*, *J. Mater. Sci.* **24** (1989) 877.
7. K. ISHIZUKA, *Acta Cryst.* **A38** (1982) 773.



*Received 6 July*
*and accepted 12 December 1989*